Organic & Biomolecular Chemistry

PAPER

View Article Online
View Journal | View Issue

Cite this: *Org. Biomol. Chem.*, 2016, **14**, 4865

The impact of α-hydrazino acids embedded in short fluorescent peptides on peptide interactions with DNA and RNA†

Josipa Sućˌ[a] Lidija-Marija Tumir,[a] Ljubica Glavaš-Obrovac,[b] Marijana Jukić,[b] Ivo Piantanida*[a] and Ivanka Jerić*[a]

Received 24th February 2016,
Accepted 25th April 2016

DOI: 10.1039/c6ob00425c

www.rsc.org/obc

A series of novel hydrazino-based peptidomimetics and analogues comprising N-terminal lysine and C-terminal phenanthridinyl-L-alanine were prepared. The presented results demonstrate the up to now unknown possibility to finely modulate peptide interactions with DNA/RNA by α-hydrazino group insertion and how the different positioning of two α-hydrazino groups in peptides controls binding to various double stranded and single stranded DNA and RNA. All peptidomimetics bind with 1–10 micromolar affinity to ds-DNA/RNA, whereby the binding mode is a combination of electrostatic interactions and hydrophobic interactions within DNA/RNA grooves. Insertion of the α-hydrazino group into the peptide systematically decreased its fluorimetric response to DNA/RNA binding in the order: mono-hydrazino < alternating-hydrazino < sequential-hydrazino group. Binding studies of ss-polynucleotides suggest intercalation of phenanthridine between polynucleotide bases, whereby affinity and fluorimetric response decrease with the number of α-hydrazino groups in the peptide sequence. Particularly interesting was the interaction of two sequential α-hydrazino acids-peptidomimetic with poly rG, characterised by a specific strong increase of CD bands, while all other peptide/ssRNA combinations gave only a CD-band decrease. All mentioned interactions could also be reversibly controlled by adjusting the pH, due to the protonation of the fluorophore.

Introduction

Life is characterised by an extremely complex system of interactions between proteins, DNA, RNA, and many small molecules. These interactions frequently take place at structurally well-defined regions formed by protein backbone folding. There is great interest in mimicking folded protein epitopes using small molecules,[1,2] biologically active peptides,[3] cyclic peptides,[4,5] or peptidomimetics.[6,7] While short peptides comprising α-amino acids generally fail to form thermodynamically stable secondary structures, backbone extended peptidomimetics comprising β- or γ-amino acids, aminoxy or hydrazino acids readily adopt "protein-like" secondary structures, such as helices, sheets and turns.[8,9] β-Peptides and oligomers containing mixtures of α- and β-amino acids have been extensively studied as inhibitors of protein–protein interactions.[10–12] Replacement of a Cβ atom in β-amino acids with nitrogen leads to hydrazino peptides, a class of peptidomimetics characterized by an array of intramolecular hydrogen bonds that are responsible for various secondary structures.[8,13,14] Although hydrazino-based peptidomimetics showed promising biological activities,[15,16] their wider exploitation is hampered by somewhat challenging synthesis. However, it has been shown recently by our group and others[17] that unprotected hydrazino acids can be successfully applied in the synthesis of hybrid hydrazino peptidomimetics, thus enabling progress in utilization of this class of compounds.

A number of short natural and synthetic peptides target DNA/RNA, among which condensed aromatic–peptide conjugates attracted quite a lot of attention in the last decade.[18] In general, the condensed-aromatic part contributed to DNA/RNA binding by intercalation and was responsible for spectrophotometric monitoring of the interaction. However, selectivity was usually controlled by the hydrogen bonding pattern along the peptide backbone within one of the DNA/RNA grooves.[18,19] To the best of our knowledge, hydrazino acids were never incorporated within DNA/RNA targeting compounds, although the

[a]*Division of Organic Chemistry and Biochemistry, Ruđer Bošković Institute, Bijenička cesta 54, 10000 Zagreb, Croatia. E-mail: pianta@irb.hr, ijeric@irb.hr*
[b]*Department of Medicinal Chemistry and Biochemistry, School of Medicine Osijek, 31000 Osijek, Croatia*

† Electronic supplementary information (ESI) available: NMR and HRMS spectra of **1–4**, spectroscopic properties (UV/Vis and fluorescence spectra), interactions of **1–4** with DNA/RNA (thermal denaturation experiments, fluorimetric titration curves, CD spectra), and cytotoxicity data. See DOI: 10.1039/c6ob00425c

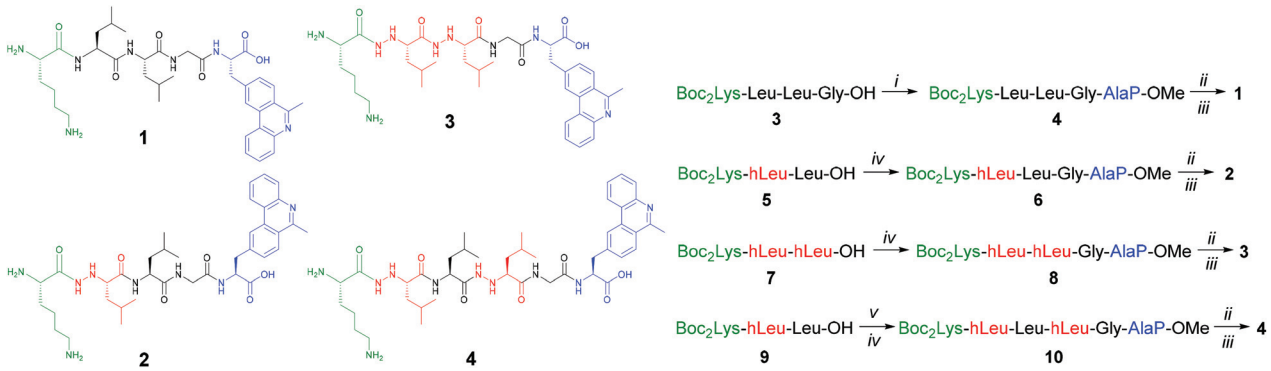

Fig. 1 Structures of hydrazino peptides (left) and preparation outline (right): (i) HATU, NMM, H-AlaP-OMe in DMF, 24 h, RT; (ii) 1 M NaOH, MeOH, 65 °C, 2 h; (iii) TFA : H_2O = 9 : 1, RT, 1 h; (iv) HATU, NMM, H-Gly-AlaP-OMe in DMF, 24 h, RT; (v) DCC, HOSu, H-hLeu-OH, in DMF, 24 h, RT.

hydrazino moiety is a well-directed double hydrogen donor. Moreover, incorporation of one or more hydrazino-based residues within short peptides can affect the peptide secondary structure. Acherar *et al.* found that, owing to the H-bond donor and acceptor character of amidic NH, hybrid oligomers composed of α-amino and α-hydrazino acids can adopt multiple conformations.[14] We presumed that such conformational adaptability could be important for steric control and preorganisation before binding to DNA/RNA. To address the aforesaid features, we prepared a small series of hydrazino-based peptidomimetics, **1–4** (Fig. 1), whereby the number and position of α-hydrazino residues are systematically varied, while keeping constant the position of positively charged lysine (expected to contribute to the DNA/RNA binding by electrostatic interactions), and fluorescent phenanthridinyl-L-alanine (AlaP) (contributing to DNA/RNA binding and reporting the recognition by fluorescence).

Results and discussion

Synthesis

Peptides comprising single hydrazino-L-leucine (hLeu) residue (**2**), two sequential hLeu residues (**3**) and alternating residues (**4**) were prepared by a solution-phase methodology. Pentapeptide **1** with incorporated AlaP was prepared to distinguish contributions of a large condensed aromatic unit and hydrazino acids on binding. Generally, peptidomimetics were prepared by a fragment assembly strategy (Fig. 1). Tripeptides **5**, **7** and **9** were synthesized according to previously developed methodologies,[17a] and coupled to a C-terminal dipeptide comprising AlaP. In the final step, terminal protecting groups were cleaved and crude products were purified by HPLC.

Physical–chemical and spectroscopic properties of aqueous solutions of 1–4

Studied compounds **1–4** are soluble in redistilled water (up to $c = 1 \times 10^{-2}$ M), and aqueous solutions were stable over 6 months. Absorbances of **1–4** aqueous solutions were proportional to their concentrations up to $c = 2\text{–}4 \times 10^{-5}$ M and didn't change notably up to 90 °C, indicating that there is no significant inter- or intramolecular aromatic stacking, which should give rise to hypochromicity effects. Fluorescence emissions of **1–4** were linearly dependent on their concentrations up to $c = 6 \times 10^{-6}$ M. Spectroscopic characterisation is given in the ESI (Fig. S1–S18†). It is noteworthy that at pH 5 the phenanthridine moiety is mostly protonated, which influences to some extent the spectroscopic properties of **1–4**, in line with previous data.[20,21] Studies of interactions with DNA and RNA were conducted at both pH 7 and pH 5 acidic conditions yielding stronger effects and thus are discussed in detail within the manuscript.

DNA/RNA binding studies

Here used AlaP was previously combined with amino acids (Gly and thyminyl-L-alanine, AlaT) and a simple dipeptide (Gly–Gly) to give moderate binding effects on ds-DNA/RNA thermal stability and CD properties.[22] The incorporation of hydrazino acid(s) at various positions in a peptide flanked by lysine on one side (for electrostatic attraction with the DNA/RNA backbone) and by AlaP on the opposite side, was expected to have a significant impact on the positioning and binding of the phenanthridine chromophore to ds-DNA/RNA. Indeed, at both pH 5 and pH 7, **1–4** didn't thermally stabilise any ds-DNA/RNA (Table S1, Fig. S19–S21†). Therefore, intercalative binding mode (common for AlaP[22]) can be excluded. To gain better structural insight into **1–4**/ds-DNA/RNA complexes, we used CD spectroscopy as a highly sensitive method for conformational changes in the secondary structure of polynucleotides.[23] Moreover, small molecule chromophores (*e.g.* AlaP in **1–4**), could upon binding to DNA or RNA acquire an induced (I)CD spectrum, which could be helpful for determination of binding modes (intercalation, groove binding, agglomeration, *etc.*).[24,25] However, negligible changes in the CD spectra of ds-polynucleotides (Fig. S23–S34†) and the absence of any induced (I)CD bands >300 nm, pointed out that the phenanthridine-chromophore does not bind in one well-defined orientation in respect of the DNA/RNA chiral axis. However, fluorimetric response (Fig. 2, ΔI in Table 1, Fig. S51–S54 ESI†) and also binding affinity (K_s, Table 1) of **1–4** to ds-DNA/RNA

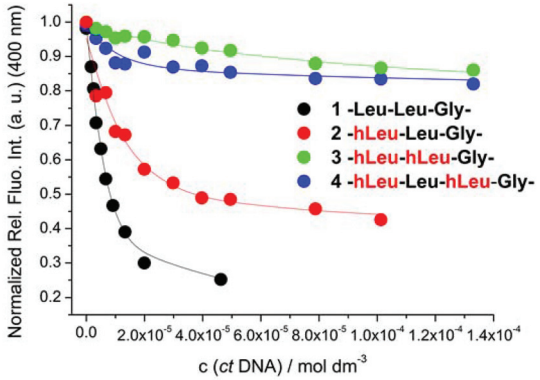

Fig. 2 Experimental (●) and calculated (–) (by Scatchard eq., Table 1) fluorescence intensities of compounds **1–4** upon addition of ct-DNA; note various positions of hydrazino-L-leucine (hLeu); Na-cacodylate buffer, pH 5.0, I = 0.05 M, λ_{exc} = 310 nm.

Table 1 Stability constants ($\log K_s$)[a] and spectroscopic properties of complexes ΔI[b] of **1–4** with ds-polynucleotides calculated according to fluorimetric titrations (Na-cacodylate buffer, c = 0.05 M, pH = 5.0; λ_{exc} = 310 nm, λ_{em} = 350–500 nm, c(**1–4**) = 1–2 × 10^{-6} M)

	ct-DNA $\log K_s$ [a]/ΔI[b]	Poly(dA–dT)$_2$ $\log K_s$ [a]/ΔI[b]	Poly(dG–dC)$_2$ $\log K_s$ [a]/ΔI[b]	Poly A–Poly U $\log K_s$ [a]/ΔI[b]
1	6.5/−78%	6.4/−80%	6.4/−81%	5.9/−75%
2	6.2/−55%	6.1/−61%	6.1/−62%	5.9/−38%
3	5.1/−20%	5.1/−21%	4.9/−35%	[c]
4	>6[d]/−12%	6.1/−24%	5.9/−34%	5–6[d]/−15%

[a] Processing of titration data by using the Scatchard equation[26] gave values of a ratio $n_{[bound\ peptide]/[polynucleotide]}$ = 0.15 ± 0.05 for most complexes; for easier comparison values of $\log K_s$ are recalculated for fixed n = 0.15; correlation coefficients were >0.98–0.99 for all calculated K_s. [b] Changes of fluorescence of compounds **1–4** induced by complex formation ($\Delta I = (I_{lim} - I_0) \times 100/I_0$; where I_0 is the emission intensity of the free compound and I_{lim} is the emission intensity of a complex calculated by using Scatchard eq.). [c] Too small and linear fluorescence change hampered the calculation of K_s. [d] Small total emission change allowed only the estimation of K_s.

were both strongly sensitive to the number of hydrazino groups in the peptide. What's more, peptidomimetic **3** with two adjacent hydrazino acids showed a lower binding affinity as well as smaller fluorescence response than peptidomimetic **4** with an alternating distribution of hydrazino acids. Also, binding constants were an order of magnitude higher at pH 5 (Table 1) than at pH 7 (Table S2, ESI†) due to the protonation of the phenanthridine moiety under acidic conditions, an additional positive charge contributing to the electrostatic component of binding.[20]

All afore-mentioned observations suggest that **1–4** bind externally to ds-DNA/RNA, whereby binding forces are not exclusively electrostatic: two positive charges (Lys and AlaP) should give $\log K_s < 4$ [27] and only four and more positive charges could yield $\log K_s \geq 6$.[28] This supports the significant contribution of hydrophobic interactions of both, the neutral peptide linker and large aromatic fluorophore, whereby the better part of the molecule is buried within the hydrophobic DNA/RNA grooves. The hydrophobic binding contribution in combination with various steric properties of hydrazino-residues is significant since it controls the position of the fluorophore yielding differences in fluorimetric response (**1** > **2** > **4** > **3**) and binding affinity.

Comparison of all obtained results revealed that the presence of Nα-unsubstituted hLeu impairs the interactions of **2–4** (compared to **1**) by withdrawing the fluorophore from the DNA/RNA binding site. When more exposed to water and less in binding contact with DNA/RNA, AlaP fluorescence is less quenched. The explanation for such an outcome can be found in conformational preferences of peptides with incorporated α-hydrazino acids, which are able to self-organize through an intramolecular hydrogen bonding network in solution. For instance peptides with Nα-substituted hydrazino acids show "hydrazino-turns", eight-membered hydrogen-bonded pseudocycles.[29,30] Furthermore, the CD spectra of the terminally protected hydrazino hexamer composed of hLeu and hAla resembles structural characteristics of β-peptides, namely the right-handed helical secondary structure.[31] Acherar *et al.* undertook in-depth secondary structure analysis of oligomers composed of alternating α-amino acids and Nα-unsubstituted hydrazino acids and reported that the major conformer present is in equilibrium between the pseudospiranic and hydrazino-turn conformation.[14]

Detailed analysis of **1–4**/DNA complexes by a structurally more informative method like NMR spectroscopy was hampered by severe peak overlapping of amide and hydrazino protons (similar as noted by Lelais and Seebach)[31] as well as insufficient solubility of compound complexes with DNA/RNA.

Molecular modelling in water of such peptides and their DNA/RNA complexes is very demanding task due to the high flexibility of peptides and mutual changing of the structure upon binding; therefore full profile modelling is out of the scope of this work. However, in an attempt to at least visualise the structural features which could explain our experimental results, we submitted **1–4** to MM2 calculations by a modified version of Allinger's MM2 force field, integrated into the ChemBio3D 11.0 programme, whereby the obtained structures (Fig. S65†) demonstrate the possible intramolecular H-bond network for each peptide, and the resulting secondary structure. It is noteworthy that structures of **1** and **2** overlap excellently (Fig. S66†), as well as the structures of bis-hydrazino **3** and **4** (Fig. S67†), however the differences between these two groups are substantial. Since compounds **1–4** do not alter the ds-DNA secondary structure (no change in DNA CD spectra, no thermal stabilisation), we used as ds-DNA model the alternating dAdT–dAdT sequence constructed earlier.[32] Manual docking of **1** and **3** was performed by using the VMD programme,[33] whereby the conformational space of small molecules within the DNA-binding site was checked and it was found that the VdW radii of the DNA and ligand did not overlap.

For **1**/DNA complex (Scheme 1, up) it is noteworthy that red lines positioned along a longer axis of AlaP and Leu/Lys chains converge into an AT-DNA minor groove, giving an excellent fit.

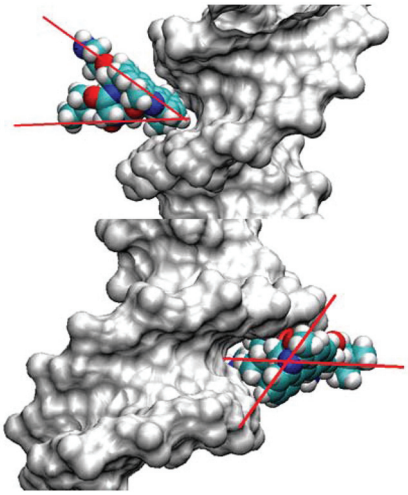

Scheme 1 Schematic presentation of **1** (up) and **3** (down) manually docked into the poly dAdT–poly dAdT minor groove. Red lines mark axes positioned along voluminous substituents: AlaP and Leu/Lys chains.

The hydrophobic area (AlaP + Leu) is pointed inside the groove, while the hydrophilic part (Lys) is pointed out. At variance with **1**, in **3**/DNA (Scheme 1, down) red lines positioned along the longer axis of AlaP and two hLeu side-chains are almost perpendicular, which hampers deep insertion of the molecule into the AT-DNA minor groove. Consequently, the fluorophore (AlaP) of **1** (and also analogue **2**) could be significantly inserted deeper into the DNA minor groove, yielding therefore a much stronger fluorimetric change in comparison to **3** and **4**.

Study of interactions of 1–4 with single stranded (ss) polynucleotides

Single stranded (ss) polynucleotides are considerably more flexible than double stranded polynucleotides.[34] However, it should be noted that both poly rA and poly rC can form double stranded partially protonated helical structures at pH 5 (namely poly rAH^+–poly rAH^+ and poly rCH^+–poly rC).[34] Also, poly rG can form complex intrastrand structures and actually only poly rU can be considered as mostly single stranded under all conditions.

Again, the fluorimetric response (Fig. 3, ΔI in Table 2 and Fig. S56–S63, ESI†) and also the binding affinity (K_s, Table 2) of **1–4** to ss-RNA were strongly sensitive to the number and distribution of hydrazino residues in the peptide with a similar tendency observed for ds-DNA/RNA (Fig. 2).

Affinities of **1–4** toward single stranded polynucleotides were similar at pH 5 (Table 2) and pH 7 (Table S3, ESI†), thus not depending on the AlaP protonation state. Since aromatic stacking interactions are usually not dependent on the aryl-charge, this suggested the intercalation of AlaP between polynucleotide bases. This was additionally supported by significantly stronger fluorescence quenching of all peptides with poly rA, poly rG compared to poly rU, poly rC polynucleotides (Table 2), attributed to more efficient aromatic stacking interactions between AlaP and larger purine nucleobases with respect to smaller pyrimidines. Again, the number and vicinity of hydrazino groups affect the affinities and fluorimetric responses in the order **1** > **2** > **4** > **3** (Fig. 3 and Fig. S56–S63, ESI†).

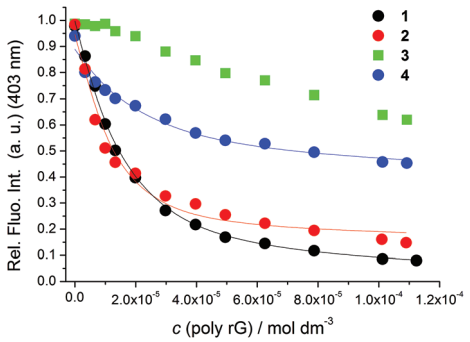

Fig. 3 Experimental (●) and calculated (–) (by Scatchard eq., Table 2) fluorescence intensities of compounds **1–4** upon addition of poly G; values were normalized for easier comparison. Na-cacodylate buffer, pH 5.0, I = 0.05 M, λ_{exc} = 310 nm.

Table 2 Stability constants ($\log K_s$)[a] and spectroscopic properties of complexes ΔI[b] of **1–4** with ss-polynucleotides calculated according to fluorimetric titrations (Na-cacodylate buffer, c = 0.05 M, pH = 5.0; λ_{exc} = 310 nm, λ_{em} = 350–500 nm, c(**1–4**) = 1–2 × 10^{-6} M)

	Poly A $\log K_s$[a]/ΔI[b]	Poly G $\log K_s$[a]/ΔI[b]	Poly U $\log K_s$[a]/ΔI[b]	Poly C $\log K_s$[a]/ΔI[b]
1	5.3/−64%	5.9/−98%	>6[c]/−12%	>6[c]/−19%
2	5.9/−42%	6.2/−82%	>5[c]/−10%	>6[c]/−9%
3	5.3/−10%	[d]	[d]	[d]
4	5–6[c]/−12%	5.7/−53%	5–6[c]/−5%	5–6[c]/−8%

[a] Processing of titration data by using the Scatchard equation[26] gave values of a ratio $n_{[bound\ peptide]/[polynucleotide]}$ = 0.15 ± 0.05 for most complexes; for easier comparison values of $\log K_s$ are recalculated for fixed n = 0.15; correlation coefficients were >0.98–0.99 for all calculated K_s. [b] Changes of fluorescence of compounds **1–4** induced by complex formation ($\Delta I = (I_{lim} - I_0) \times 100/I_0$; where I_0 is the emission intensity of the free compound and I_{lim} is the emission intensity of a complex calculated by using Scatchard eq.). [c] Small total emission change allowed only the estimation of K_s. [d] Too small and linear fluorescence change/no fluorescence change hampered the calculation of K_s.

CD spectropolarimetry was applied for detailed structural analysis of complexes.[24,25] Under acidic conditions (pH 5, protonated AlaP) addition of **1–4** resulted in much stronger CD response of ss-RNA (Fig. 4 and 5) with respect to pH 7 (Fig. S35–S50, ESI†), thus only the results obtained at pH 5 are further discussed.

The minor decrease within the 250–300 nm region could be attributed to intercalation of phenanthridine, which should yield a weak negative ICD band[25] around its absorption maximum (250 nm, Fig. 4) as well as deformation of the polynucleotide helical structure causing a general RNA-CD band decrease.[23,25] Both expected changes could explain the observed decrease of the CD spectra upon formation of poly rA/**1–4** complexes (Fig. S35–38†) and poly rG/**1**, **2**, **4** complexes (Fig. 4). Also, the less pronounced decrease in poly rU and poly

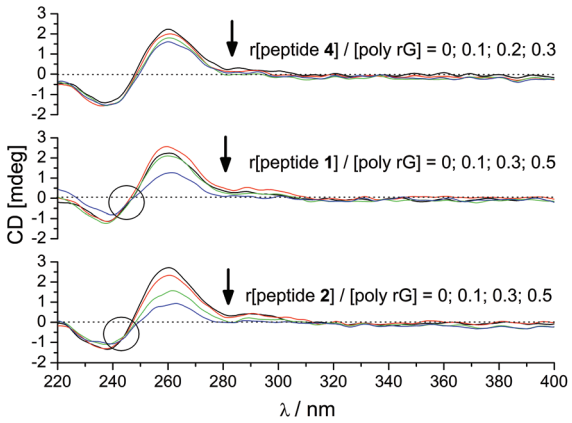

Fig. 4 CD titration of poly G (c = 2 × 10^{-5} M) with **1**, **2**, and **4** at different molar ratios r = [compound]/[poly G]. Note the isodichroic point in the circle. Done at pH = 5.0, sodium cacodylate buffer, I = 0.05 M.

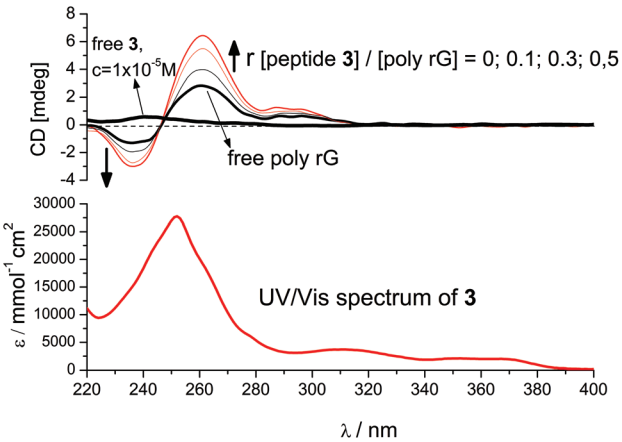

Fig. 5 CD titration of poly G (c = 2 × 10^{-5} M) with **3** at different molar ratios r = [compound]/[poly G]. Note the isodichroic point in the circle. Done at pH = 5.0, sodium cacodylate buffer, I = 0.05 M.

rC complexes could be attributed to the smaller nucleobase size and consequently less-efficient aromatic stacking with phenanthridine.

However, as a unique exception, peptidomimetic **3** yielded a strong increase of all CD bands (Fig. 5), whereby the isoelliptic point in poly rG/**3** titration strongly supported the formation of only one type of a complex.

Throughout the study presented here, **3** showed the lowest fluorescence increase for all ds-DNA/RNA and in particular for most ss-RNA, which could be attributed to the rigidity of the peptide structure due to two sequential hLeu residues. Since hydrazino peptides can be considered an extension of the β-peptide concept, possible secondary structures of hydrazino peptides can be compared with those of β-peptides.[35] It is well documented that systematic combination of α- and β-amino acids generates new secondary structures.[36–38] Thus, mixed α/β peptides were found to adopt various helical secondary structures, depending on the chirality, structure and distribution of two structural units. Generally, introduction of α-amino acids increases flexibility compared with homogeneous β-peptides,[35] therefore it can be presumed that peptide **3** with two sequential hLeu residues is more rigid than **2** and **4** with an alternating distribution of Leu and hLeu. Thus, the observed strong CD spectrum increase (Fig. 5) could be attributed to the switch of the binding mode of the poly rG/**3** complex, whereby phenanthridine is not intercalated (as in other ss-RNA) due to steric constraints of two sequential hLeu residues but likely positioned along the poly rG chain. Such arrangement could increase RNA chirality by stabilizing the helical structure of otherwise not-well organized ss-RNA (thus increasing RNA CD bands) and moreover is likely to be combined with a strong positive ICD band of chromophore bound at an approximately 45° angle to the RNA chiral axis.[25] Most intriguingly, at pH 7 such an increase of the poly rG CD spectrum by **3** was much weaker, and didn't change the negative band at 240 nm (ESI†) pointing out that protonation of phenanthridine plays a crucial role, most likely due to electrostatic interactions with the negatively charged phosphate backbone (another proof of non-intercalative binding).

Biology

While mixed α/β-peptides are widely exploited for studying the inhibition of protein–protein interactions (PPI),[39–42] hydrazino-based peptidomimetics were used to a much lesser extent, mainly as human leukocyte elastase and proteasome inhibitors,[15] or antimicrobial agents.[16] Keeping in mind that many PPIs are mediated by small peptides, the use of designed peptides and peptidomimetics not only as modulators of PPI is recognized as a promising strategy in drug discovery, but also as probes to elucidate the role of PPI in cell biology.[43]

Phenanthridinium derivatives are often strongly cytotoxic, which renders their applications as dyes in biochemical studies on DNA and RNA.[44] Short peptides also could show considerable cell toxicity. However, both phenanthridine analogues[45] and peptides are studied as powerful anticancer drugs. For this reason we screened compounds **1**, **2** and **4** for cytotoxic activity against two adenocarcinoma cell lines: cervix (HeLa) and colon (CaCo-2), chronic myeloid leukaemia in blast crisis (K562), and normal epithelial cell line (MDCK1) as well. Results pointed out negligible activity of all studied peptidomimetics (ESI, S64†) that reached growth inhibition by 50% (GI_{50}) just on K562 cells at a concentration near or higher than 10^{-4} M. Such low cytotoxicity makes these fluorescent peptides safe dyes for laboratory applications.

Conclusions

Hydrazino peptidomimetics **1–4** were prepared to study systematically the impact of hydrazino-L-leucine (hLeu) residues in a short peptide sequence linking two common DNA/RNA-interacting moieties: positively charged lysine at the peptide

N-terminal part and phenanthridinyl-L-alanine (AlaP) at the peptide C-terminal part, acting as pH-dependent fluorophores.

Comparison of results obtained for **1–4** with those reported previously for dipeptides Gly-AlaP and thyminyl-L-alanyl-phenanthridinyl-L-alanine (AlaT-AlaP)[22] revealed that the N-terminal peptide part has great influence on the binding mode. Already the Lys-Leu-Leu-Gly sequence in **1** caused switch of the binding ds-DNA/RNA mode from intercalation, reported for Gly-AlaP and AlaT-AlaP,[22] to external binding combined with the polynucleotide groove interaction. Moreover, replacement of leucine with hydrazino analogues, their number and distribution along the peptide backbone determined binding to ds-DNA/RNA, which was proportionally reported by quenching of AlaP fluorescence in the order: **2** (single hLeu) > **4** (two alternating hLeu) > **3** (two sequential hLeu). In addition, all peptides retained moderate (1–10 μM) affinity toward ds-DNA/RNA, externally controllable by pH (due to AlaP protonation) by change in the order of magnitude. Intriguingly, peptides **1–4** showed high affinity toward ss-RNA (comparable to ds-DNA/RNA). Again, the fluorimetric response of AlaP was proportional to the number of hLeu in the peptide sequence, *i.e.* emission quenching tendency decreased in the order **1** > **2** > **4** > **3**.

However, the most interesting was the specific binding of peptide **3** with two sequential hLeu to poly rG, which caused unique super-organisation of poly rG characterised by specific response in the CD spectrum. In addition, CD response at 240 nm (negative band attributed to the poly rG backbone) was observed only at pH 5 but not pH 7, and thus could be switched on and off by non-destructive external stimuli (pH). Such a specific spectrophotometric probe for micromolar concentrations of poly rG is to the best of our knowledge not known.

The presented results demonstrate the up to now untried possibility to finely modulate the peptide interaction with DNA/RNA by α-hydrazino-group insertion and moreover the combination of several α-hydrazino-groups within the peptide. The given results (along with non-toxicity of these peptidomimetics) encourage further studies in line with the combination of multiple α-hydrazino-groups within the peptide to completely abolish ds-DNA/RNA binding and still preserve high ss-DNA/RNA affinity with particular emphasis on specific poly G recognition achieved by **3**. This future research would directly address a very limited number of small molecules highly selective or specific toward ss-DNA/RNA sequences, which have found intriguing biomedical uses, for instance in antiviral and antitumor applications.[46,47] Although there are examples of peptides binding to ss-DNA,[48] intriguingly, ss-RNA were strongly underexploited targets, most likely due to a larger variety of biologically available forms.[49,50]

Experimental section

Materials and methods

Reactions were monitored by TLC on Silica Gel 60 F254 plates (Merck; Darmstadt, Germany) upon detection with ninhydrin. Column chromatography was performed on silica gel (Merck, 0.040–0.063). RP HPLC analysis was performed on a HPLC system coupled with a UV detector; a C-18 semipreparative (250 9 8 mm, ID 5 μm) column at a flow rate of 1 mL min^{-1}, or an analytical (150 9 4.5 mm, ID 5 μm) column at a flow rate of 0.5 mL min^{-1}. UV detection was performed at 254 nm or 270 nm. NMR spectra were recorded on 600 and 300 MHz spectrometers, operating at 150.92 or 75.47 MHz for ^{13}C and 600.13 or 300.13 MHz for ^{1}H nuclei. TMS was used as an internal standard. Mass spectrometry measurements were performed on a HPLC system coupled with a triple quadrupole mass spectrometer, operating in positive electrospray ionization (ESI) mode. Spectra were recorded from a 10 μg per mL compound solution in 50% MeOH/0.1% FA by injection of 3 μL into the ion source of the instrument by using an autosampler, at a flow rate of 0.2 mL min^{-1} (mobile phase 50% MeOH/0.1% FA). HRMS analysis was performed on a MALDI-TOF mass spectrometer operating in reflectron mode. Mass spectra were acquired by accumulating three spectra after 400 laser shots per spectrum. Calibrant and analyte spectra were obtained in positive ion mode. Calibration type was internal with calibrants produced by matrix ionization (monomeric, dimeric and trimeric CHCA), with azithromycin and angiotensin II dissolved in the α-cyano-4-hydroxycinnamic acid matrix in the mass range m/z 190.0499 to 749.5157 or 1046.5417. Accurately measured spectra were internally calibrated and elemental analysis was performed on Data Explorer v. 4.9 software with mass accuracy better than 5 ppm. Samples were prepared by mixing 1 μL of analyte methanol solution with 5 μL of saturated (10 mg mL^{-1}) solution of α-cyano-4-hydroxycinnamic acid (α-CHCA) and internal calibrants (0.1 mg mL^{-1}) dissolved in 50% acetonitrile/0.1% TFA. MM2 calculations were performed by using a modified version of Allinger's MM2 force field, integrated into the ChemBioOffice 2008 programme. Compounds **3**, **5**, **7** and **9** were prepared according to a previously developed procedure.[17a]

All measurements were performed in an aqueous buffer solution (pH = 5, I = 0.05 M, sodium cacodylate/HCl buffer or pH = 7, I = 0.05 M, sodium cacodylate/HCl buffer). The UV-Vis spectra were recorded on a Varian Cary 100 Bio spectrometer in quartz cuvettes (1 cm). Fluorescence spectra were recorded on a Varian Cary Eclipse fluorimeter in quartz cuvettes (1 cm). Under the experimental conditions used (~10^{-6} M) the absorbance and fluorescence intensities of **1–4** were proportional to their concentrations.

Polynucleotides were purchased as noted: poly dGdC–poly dGdC, poly dAdT–poly dAdT, poly A–poly U, poly A, poly G, poly U, poly C (Sigma), calf thymus (ct)-DNA (Aldrich) and dissolved in sodium cacodylate buffer, I = 0.05 M, pH = 7. The calf thymus ctDNA was additionally sonicated and filtered through a 0.45 mm filter.[51] The polynucleotide concentration was determined spectroscopically[52] as the concentration of phosphates. The concentration of the stock solution (10 mM) of single stranded poly A at pH 7 was determined by UV absorbance measurement at 258 nm using a molar extinction coefficient (ε) value of 9800 M^{-1} cm^{-1} and it was expressed as the

concentration of phosphates. It is important to note that under experimental conditions (pH = 5) poly A and poly C were protonated and formed a double helix. The double-stranded conformation of poly A and poly C was obtained by lowering the pH value from the initial value of 7.0 to 5.0 and their concentrations were directly derived from the concentration of single stranded polynucleotides (ss-poly A). The formation of ds-poly A and ds-poly C was confirmed by CD and thermal melting experiments.[53,54]

In fluorimetric experiments, excitation wavelengths at $\lambda_{max} \geq 305$ nm were used in order to avoid absorption of excitation light by added polynucleotides. Fluorimetric titrations were performed by adding portions of the polynucleotide solution into the solution of the studied compound ($c = 2 \times 10^{-6}$ M). After mixing polynucleotides with studied compounds it was observed in all cases that equilibrium was reached in less than 120 seconds. In following 2–3 hours the fluorescence spectra of complexes remained constant. Fluorescence spectra were collected at $r < 0.3$ (r = (compound)/(polynucleotide)) to assure one dominant binding mode. Data that were processed by means of the Scatchard equation[26] gave values of a ratio n [bound compound]/[polynucleotide] in the range 0.07–0.2, but for easier comparison all K_s values were re-calculated for fixed $n = 0.15$. Calculated values for K_s have satisfactory correlation coefficients (>0.99).

CD spectra were recorded on a JASCO J815 spectrophotometer at room temperature using appropriately 1 cm path quartz cuvettes with a scanning speed of 200 nm min^{-1}. The buffer background was subtracted from each spectrum, while each spectrum was a result of three accumulations. CD experiments were performed by adding portions of the compound stock solution into the solution of polynucleotide (c = 1–2 × 10^{-5} M).

Thermal melting experiments were performed on a Varian Cary 100 Bio spectrometer in quartz cuvettes (1 cm). The measurements were done in aqueous buffer solution at pH 5 or pH 7 (sodium cacodylate/HCl buffer $I = 0.03$ M). Thermal melting curves for ds-DNA, ds-RNA and their complexes with **1–4** were determined by following the absorption change at 260 nm as a function of temperature.[55,56] The absorbance scale was normalized. T_m values are the midpoints of the transition curves determined from the maximum of the first derivative and checked graphically by the tangent method. The ΔT_m values were calculated subtracting T_m of the free nucleic acid from T_m of the complex. Every ΔT_m value here reported was the average of at least two measurements. The error in ΔT_m is ±0.5 °C.

Synthetic procedures

Boc-Lys(Boc)-Leu-Leu-Gly-AlaP-OMe (4). Boc-Lys(Boc)-Leu-Leu-Gly-OH (**3**) (32 mg, 0.051 mmol) was dissolved in dry DMF, and then NMM (8 μL, 0.051 mmol) and HATU (22 mg, 0.056 mmol) were added and the reaction mixture was stirred at room temperature. After 15 min a solution of H-AlaP-OMe (20 mg, 0.051 mmol) and NMM (8 μL, 0.051 mmol) in 2 mL dry DMF was added. The reaction mixture was stirred at room temperature overnight. The solvent was evaporated and the residue was purified by the flash column chromatography in EtOAc : petroleum ether : EtOH 3 : 1 : 0.5.

Yield: 54% (25 mg). Yellow oil. R_f 0.77 (EtOAc : petroleum ether : EtOH 3 : 1 : 0.5). M_r 906.12. ESI-MS: m/z 906.5 $[M + H]^+$. ^{1}H NMR (600 MHz, CD_3OD): δ 7.63–7.56 (m, 7H H_{ar} AlaP), 4.89 (m, 1H, α AlaP), 4.10 (m, 1H, α Lys), 3.96–3.82 (m, 2H, α Leu^2, Leu^3), 3.74 (s, 2H, α Gly), 3.35 (s, 3H, OCH_3), 3.06 (m, 2H, β AlaP), 3.03 (m, 2H, ε Lys), 1.73–1.55 (m, 10H, β,δ Lys, β,γ Leu^2, Leu^3), 1.45–1.42 (m, 18H, CH_3 Boc), 1.33 (m, 2H, γ Lys), 0.99–0.94 (m, 6H, δ,δ′ Leu^2), 0.90–0.84 (m, 6H, δ,δ′ Leu^3).

H-Lys-Leu-Leu-Gly-AlaP-OH (1). Compound **4** (46 mg 0.051 mmol) was dissolved in 5 mL of methanol and 1 M NaOH (105 μL, 0.105 mmol) was added. The reaction mixture was stirred under reflux for 2 h. The solvent was evaporated, the residue was dissolved in water, acidified to pH 3 by using 10% citric acid and the product was extracted with EtOAc. After solvent evaporation, the residue was dissolved in 0.5 mL of a TFA–H_2O mixture (9 : 1, v/v) and the reaction mixture was stirred at room temperature for 1 h. The solvent was evaporated and the product was purified by RP-HPLC. HPLC conditions: Eurospher 100 RP C-18 column 250 × 4.5 mm, i.d. 5 μm; flow rate = 1 mL min^{-1}; λ = 270 nm; mobile phase: 0 min 40% B, 0–20 min 40% B-90% A, 20–30 min 90% B, 30–35 min 90% B-40% B. A = 0.1% TFA in water, B = 0.1% TFA in MeOH.

Yield: 67% (12 mg). Colorless oil. R_t 19.0 min. M_r 691.86. ESI-MS: m/z 346.8 $[M + H]^{2+}$, m/z 692.4 $[M + H]^+$. ^{1}H NMR (600 MHz, CD_3OD): δ 8.94 (d, J = 8.6 Hz, 1H), 8.49 (d, J = 7.5 Hz, 1H), 8.51 (m, 1H), 8.21–8.16 (m, 2H), 8.00 (d, J = 7.0 Hz, 1H), 7.96 (d, J = 6.3 Hz, 1H), 4.93 (m, 1H), 4.47 (m, 1H), 4.33–4.24 (m, 1H), 3.95 (m, 1H), 3.90–3.78 (dd, ^2J = 16.9 Hz 2H), 3.38 (s, 3H), 3.36 (s, 2H), 2.99 (m, 2H), 1.91 (m, 2H), 1.78–1.69 (m, 4H), 1.64 (m, 3H), 1.58–1.48 (m, 3H), 1.00–0.86 (m, 12H). ^{13}C NMR (151 MHz, CD_3OD): δ 174.9, 174.7, 174.2, 171.2, 170.0, 162.8, 141.1, 138.8, 138.5, 134.3, 133.7, 133.2, 132.2, 130.4, 125.8, 125.5, 125.9, 124.6, 54.7, 53.9, 53.7, 53.4, 43.2, 41.7, 41.4, 40.2, 38.6, 32.0, 28.0, 25.8, 25.7, 23.4, 23.2, 22.4, 22.0, 21.8, 20.2. HRMS (MALDI-TOF/TOF): calcd for $C_{37}H_{53}N_7O_6$ $[M + H]^+$ 692.4130; found 692.415.

Boc-Lys(Boc)-hLeu-Leu-Gly-AlaP-OMe (6). Compound **5** (85 mg, 0.14 mmol) was dissolved in dry DMF, and then NMM (15 μL, 0.14 mmol) and HATU (58 mg, 0.15 mmol) were added. After 15 min a solution of H-Gly-AlaP-OMe (65 mg, 0.14 mmol) and NMM (15 μL, 0.14 mmol) in 1 mL dry DMF was added. The reaction mixture was stirred at room temperature overnight. The solvent was evaporated and the residue was purified by flash column chromatography in EtOAc : petroleum ether : EtOH 3 : 1 : 0.5.

Yield: 22% (28 mg). Yellow oil. R_f 0.7 (EtOAc : petroleum ether : EtOH 3 : 1 : 0.5). M_r 921.13. ESI-MS: m/z 921.8 $[M + H]^+$. ^{1}H NMR (600 MHz, CD_3OD): δ 8.69 (m, 2H), 8.38 (m, 2H), 8.08 (d, J = 8.3 Hz, 1H), 7.48 (dd, ^2J = 8.4 Hz, 2H), 4.94 (m, 1H), 3.92 (m, 1H), 3.89–3.81 (m, 1H), 3.78–3.74 (m, 2H), 3.57–3.50 (m, 1H), 3.45–3.32 (m, 2H), 2.99 (s, 3H), 2.86 (s, 3H), 2.85–2.82 (m, 2H), 1.84 (m, 2H), 1.74–1.67 (m, 3H), 1.62–1.55 (m, 3H),

1.53–1.47 (m, 2H), 1.47–1.38 (m, 18H), 1.18–1.09 (m, 2H), 1.00–0.80 (m, 12H).

H-Lys-hLeu-Leu-Gly-AlaP-OH (2). Compound **6** (60 mg 0.07 mmol) was dissolved in 5 mL of methanol and 1 M NaOH (130 μL; 0.13 mmol) was added. The reaction mixture was stirred under reflux for 2 h. The solvent was evaporated, the residue was dissolved in water, acidified to pH 3 by using 10% citric acid and the product was extracted with EtOAc. After solvent evaporation, the residue was dissolved in 0.5 mL of a TFA–H_2O mixture (9 : 1, v/v) and the reaction mixture was stirred at room temperature for 1 h. The solvent was evaporated and the product was purified by RP-HPLC. HPLC-conditions: Eurospher 100 RP C-18 column 250 × 4.5 mm, i.d. 5 μm; flow rate = 1 mL min^{-1}; λ = 270 nm; mobile phase: 0 min 50% B, 0–20 min 50% B-90% A, 20–30 min 90% B, 30–35 min 90% B-50% B. A = 0.1% TFA in water, B = 0.1% TFA in MeOH.

Yield: 10% (5 mg). Colorless oil. R_t 16.7 min. M_r 706.87. ESI-MS: m/z 707.3 $[M + H]^+$. ^{1}H NMR (600 MHz, CD_3CN): δ 8.83–8.78 (m, 2H), 8.42 (m, 1H), 8.38 (m, 1H), 8.15 (d, J = 8.3 Hz, 1H), 7.97–7.93 (m, 2H), 7.66 (m, 2H), 7.60 (d, J = 8.8 Hz, 1H), 7.50 (m, 2H), 4.80 (m, 1H), 4.34 (m, 2H), 3.88 (s, 2H), 3.56–3.54 (m, 1H), 3.32 (m, 2H), 2.95 (s, 3H), 1.68 (m, 2H), 1.65 (m, 2H), 1.57 (m, 2H), 1.53 (m, 2H), 1.46 (m, 2H), 1.34–1.32 (m, 2H), 0.97–0.93 (m, 12H). ^{13}C NMR (151 MHz, CD_3CN): δ 176.3, 175.3, 171.2, 169.2, 169.2, 161.1, 160.9, 140.6, 138.7, 137.5, 137.2, 133.9, 132.1, 131.3, 130.5, 125.4, 125.2, 124.4, 64.4, 54.6, 52.9, 51.9, 41.2, 40.4, 40.2, 37.7, 37.5, 30.9, 26.7, 25.8, 25.7, 23.2, 23.1, 22.4, 21.9, 21.5, 21.4. HRMS (MALDI-TOF/TOF): calcd for $C_{37}H_{54}N_8O_6$ $[M + H]^+$ 707.4239; found 707.4252.

Boc-Lys(Boc)-hLeu-hLeu-Gly-AlaP-OMe (8). Compound **7** (80 mg, 0.13 mmol) was dissolved in dry DMF, and then NMM (15 μL, 0.13 mmol) and HATU (54 mg, 0.13 mmol) were added. After 15 min a solution of H-Gly-AlaP-OMe (60 mg, 0.13 mmol) and NMM (15 μL, 0.13 mmol) in 1 mL dry DMF was added. The reaction mixture was stirred at room temperature overnight. The solvent was evaporated and the residue was purified by flash column chromatography in EtOAc : petroleum ether : EtOH 3 : 1 : 0.5.

Yield: 11% (14 mg). Yellow oil. R_f = 0.82 (EtOAc : petroleum ether : EtOH 3 : 1 : 0.5). M_r 936.15. ESI-MS: m/z 937.9 $[M + H]^+$. ^{1}H NMR (300 MHz, CD_3OD): δ 8.74 (m, 1H), 8.27–8.00 (m, 1H), 7.93–7.30 (m, 5H), 4.97 (m, 1H), 4.25 (m, 1H), 4.19–3.90 (m, 1H), 3.88–3.75 (m, 1H), 3.74–3.41 (m, 2H), 3.40 (s, 3H), 3.20–2.88 (m, 4H), 2.87 (s, 3H), 2.07–1.54 (m, 8H), 1.48 (m, 18H), 1.45–1.29 (m, 4H), 1.10–0.86 (m, 12H, δ,δ′ hLeu).

H-Lys-hLeu-hLeu-Gly-AlaP-OH (3). Compound **8** (50 mg, 0.05 mmol) was dissolved in 5 mL methanol and 1 M NaOH (110 μL, 0.11 mmol) was added. The reaction mixture was stirred under reflux for 2 h. The solvent was evaporated, the residue was dissolved in water, acidified to pH 3 by using 10% citric acid and the product was extracted with EtOAc. After solvent evaporation, the residue was dissolved in 0.5 mL of a TFA–H_2O mixture (9 : 1, v/v) and the reaction mixture was stirred at room temperature for 1 h. The solvent was evaporated and the product was purified by RP-HPLC. HPLC conditions: Eurospher 100 RP C-18 column 250 × 4.5 mm, i.d. 5 μm; flow rate = 1 mL min^{-1}; λ = 270 nm; mobile phase: 0 min 50% B, 0–20 min 50% B-90% A, 20–30 min 90% B, 30–35 min 90% B-50% B. A = 0.1% TFA in water, B = 0.1% TFA in MeOH.

Yield: 13% (5 mg). Colorless oil. R_t 18.1 min. M_r 721.89. ESI-MS: m/z 722.5 $[M + H]^+$. ^{1}H NMR (600 MHz, CD_3CN): δ 8.74 (m, 2H), 8.31 (d, J = 5.3 Hz, 1H), 8.02 (d, J = 8.5 Hz, 1H), 7.20 (m, 3H), 6.65 (s, 1H), 4.82 (m, 1H), 3.77–3.70 (m, 1H), 3.68 (m, 2H), 3.54–3.49 (m, 2H), 3.32 (m, 2H), 3.26 (s, 3H), 2.54 (m, 2H), 2.04 (m, 2H), 1.87–1.80 (m, 2H), 1.63 (m, 2H), 1.56–1.50 (m, 2H), 1.38–1.32 (m, 4H), 0.89–0.86 (m, 12H). ^{13}C NMR (151 MHz, CD_3CN): δ 178.1, 172.1, 171.4, 170.9, 170.1, 162.8, 141.1, 138.8, 138.5, 134.3, 134.1, 133.7, 133.2, 132.8, 131.9, 130.4, 125.8, 125.7, 124.0, 124.6, 66.3, 63.9, 57.8, 53.6, 43.5, 41.3, 40.1, 38.6, 33.8, 29.6, 25.6, 24.8, 22.8, 22.1, 22.0, 21.9, 20.2. HRMS (MALDI-TOF/TOF): calcd for $C_{37}H_{55}N_9O_6$ $[M + H]^+$ 722.4348; found 722.4349.

Boc-Lys(Boc)-hLeu-Leu-hLeu-Gly-AlaP-OMe (10). Boc-Lys (Boc)-hLeu-Leu-hLeu-OH (45 mg, 0.063 mmol) was dissolved in dry DMF, and then NMM (7 μL, 0.063 mmol) and HATU (26 mg, 0.069 mmol) were added. After 15 min a solution of H-Gly-AlaP-OMe (30 mg, 0.063 mmol) and NMM (7 μL, 0.063 mmol) in 1 mL dry DMF was added. The reaction mixture was stirred at room temperature overnight. The solvent was evaporated and the residue was purified by flash column chromatography with eluents EtOAc : petroleum ether : EtOH = 3 : 1 : 0.5.

Yield: 61% (40 mg). Yellow oil. R_f = 0.78 (EtOAc : petroleum ether : EtOH = 3 : 1 : 0.5). M_r 1049.31. ESI-MS: m/z 1050 $[M + H]^+$.

H-Lys-hLeu-Leu-hLeu-Gly-AlaP-OH (4). Compound **9** (40 mg, 0.038 mmol) was dissolved in 5 mL methanol and 1 M NaOH (286 μL, 0.286 mmol) was added. The reaction mixture was stirred under reflux for 12 h. The solvent was evaporated, the residue was dissolved in water, acidified to pH 3 by using 10% citric acid and the product was extracted with EtOAc. After solvent evaporation, the residue was dissolved in 0.5 mL of a TFA–H_2O mixture (9 : 1, v/v) and the reaction mixture was stirred at room temperature for 1 h. The solvent was evaporated and the product was purified by RP-HPLC. HPLC conditions: Eurospher 100 RP C-18 column 250 × 4.5 mm, i.d. 5 μm; flow rate = 1 mL min^{-1}; λ = 270 nm; mobile phase: 0 min 50% B, 0–20 min 50% B-90% A, 20–30 min 90% B, 30–35 min 90% B-50% B. A = 0.1% TFA in water, B = 0.1% TFA in MeOH.

Yield: 10% (3 mg). Colourless oil. R_t 23.8 min. M_r 835.05. ESI-MS: m/z 835.6 $[M + H]^+$. ^{1}H NMR (600 MHz, CD_3OD): δ 8.97 (m, 1H), 8.79 (m, 1H), 8.51 (dd, J = 8.4 Hz, 1H), 8.27–7.99 (m, 3H), 7.56 (d, ^2J = 8.4 Hz, 1H), 4.91 (m, 1H), 4.49–4.42 (m, 1H), 4.14–4.06 (m, 1H), 3.64 (m, 2H), 3.39 (s, 5H), 3.01 (m, 2H), 2.99–2.91 (m, 2H), 2.01 (m, 2H), 1.93–1.88 (m, 2H), 1.78–1.75 (m, 3H), 1.68–1.59 (m, 12H), 1.53–1.50 (m, 2H), 0.98–0.93 (m, 18H). ^{13}C NMR (151 MHz, CD_3CN): δ 178.2, 172.3, 171.6, 170.7, 170.3, 170.1, 162.8, 141.2, 138.7, 138.6,

134.3, 133.9, 132.5, 131.8, 130.4, 125.8, 125.5, 125.1, 124.7, 124.6, 66.3, 63.7, 57.6, 57.3, 55.4, 53.5, 43.7, 41.2, 40.1, 39.8 38.6, 33.5, 32.8, 29.6, 25.8, 25.5, 24.8, 24.6, 22.7, 22.4, 22.2, 21.7, 20.3. HRMS (MALDI-TOF/TOF): calcd for $C_{43}H_{66}N_{10}O_7$ $[M + H]^+$ 835.5188; found 835.5199.

Cytotoxicity evaluation

Cytotoxic effects on the normal and tumors cells' growth were determined using the colorimetric methyltetrazolium (MTT) assay. Experiments were carried out on three tumor human cell lines (HeLa, CaCo-2, and K562) and on one canine cell line (MDCK I) as normal cells. The adherent cells, MDCK1, HeLa, and $CaCO_2$, were seeded in 96 micro-well plates at a concentration of 2×10^4 cells per mL and allowed to attach overnight in a CO_2 incubator (IGO 150 CELLlife™, JOUAN, Thermo Fisher Scientific, Waltham, MA, USA). After 72 hours of exposure to tested compounds, the medium was replaced with 5 mg mL^{-1} MTT solution and the resulting formazan crystals were dissolved in DMSO. Leukemia cells at a concentration of 1×10^5 cells per mL were plated onto 96 micro-well plates and after 72 hours of incubation, 5 mg mL^{-1} MTT solution was added to each well and incubated for 4 hours in a CO_2 incubator. To each well, 10% SDS with 0.01 mol L^{-1} HCl was added to dissolve water-insoluble MTT-formazan crystals overnight. An Elisa microplate reader (iMark, BIO RAD, Hercules, CA, USA) was used for measurement of absorbance at 595 nm. All experiments were performed at least three times in triplicate. The percentage of cell growth (PG) was calculated using the following equation:

$$\mathrm{PG} = (A_{\mathrm{compound}} - A_{\mathrm{background}}/A_{\mathrm{control}} - A_{\mathrm{background}}) \times 100$$

where $A_{\mathrm{background}}$ at the adherent cells is the absorbance of MTT solution and DMSO; $A_{\mathrm{background}}$ at the suspension cells is the absorbance of the medium without cells, but containing MTT and 10% SDS with 0.01 mol L^{-1} HCl; and A_{control} is the absorbance of the cell suspension grown without tested compounds.

Acknowledgements

This work has been supported by the Croatian Science Foundation projects 1477 and 3102. The support from the FP7-REGPOT-2012-2013-1 project, Grant Agreement Number 316289 – InnoMol is gratefully acknowledged.

Notes and references

1 Y. Zhao, A. Aguilar, D. Bernard and S. Wang, *J. Med. Chem.*, 2015, **58**, 1038.
2 A. Domling, *Curr. Opin. Chem. Biol.*, 2008, **12**, 281.
3 J. D. A. Tyndall, B. Pfeiffer, G. Abbenante and D. P. Fairlie, *Chem. Rev.*, 2005, **105**, 793.
4 T. A. Hill, N. E. Shepherd, F. Diness and D. P. Fairlie, *Angew. Chem., Int. Ed.*, 2014, **53**, 2.
5 J. M. Smith, J. R. Frost and R. Fasan, *Chem. Commun.*, 2014, **50**, 5027.
6 J. K. Murray and S. H. Gellman, *Pept. Sci.*, 2007, **88**, 657.
7 L. Nevola and E. Giralt, *Chem. Commun.*, 2015, **51**, 3302.
8 I. Avan, C. D. Hallb and A. R. Katritzky, *Chem. Soc. Rev.*, 2014, **43**, 3575.
9 P. G. Vasudev, S. Chatterjee, N. Shamala and P. Balaram, *Chem. Rev.*, 2011, **111**, 657.
10 D. Seebach and J. Gardiner, *Acc. Chem. Res.*, 2008, **41**, 1366.
11 A. D. Bautista, J. S. Appelbaum, C. J. Craig, J. Michel and A. Schepartz, *J. Am. Chem. Soc.*, 2010, **132**, 2904.
12 E. V. Denton, C. J. Craig, R. L. Pongratz, J. S. Appelbaum, A. E. Doerner, A. Narayanan, G. I. Shulman, G. W. Cline and A. Schepartz, *Org. Lett.*, 2013, **15**, 5318.
13 A. Cheguillaume, A. Salaün, S. Sinbandhit, M. Potel, P. Gall, M. Baudy-Floch and P. Le Grel, *J. Org. Chem.*, 2001, **66**, 4923.
14 S. Acherar, A. Salaün, P. Le Grel, B. Le Grel and B. Jamart-Grégoire, *Eur. J. Org. Chem.*, 2013, 5603.
15 (*a*) M. Laurencin, M. Amor, Y. Fleury and M. Baudy-Floc'h, *J. Med. Chem.*, 2012, **55**, 10885; (*b*) M. Laurencin, B. Legrand, E. Duval, J. Henry, M. Baudy-Floc'h, C. Zatylny-Gaudin and A. Bondon, *J. Med. Chem.*, 2012, **55**, 2025.
16 A. Bordessa, M. Keita, X. Maréchal, L. Formicola, N. Lagarde, J. Rodrigoa, G. Bernadat, C. Bauvais, J. L. Soulier, L. Dufau, T. Milcent, B. Crousse, M. Reboud-Ravauxb and S. Ongeri, *Eur. J. Med. Chem.*, 2013, **70**, 505.
17 (*a*) J. Sućand I. Jerić, *SpringerPlus*, 2015, **4**, 507; (*b*) S. S. Panda, C. El-Nachef, K. Bajaj and A. R. Katritzky, *Eur. J. Org. Chem.*, 2013, 4156.
18 J. Matić, L.-M. Tumir, M. Radić Stojković and I. Piantanida, *Curr. Protein Pept. Sci.*, 2016, **17**, 127.
19 (*a*) A. L. Stewart and M. L. Waters, *ChemBioChem*, 2009, **10**, 539–544; (*b*) L. L. Cline and M. L. Waters, *Org. Biomol. Chem.*, 2009, **7**, 4622–4630.
20 L.-M. Tumir, I. Piantanida, P. Novak and M. Žinić, *J. Phys. Org. Chem.*, 2002, **15**, 599.
21 L.-M. Tumir, I. Piantanida, I. Juranović, Z. Meić, S. Tomić and M. Žinić, *Chem. Commun.*, 2005, 2561.
22 (*a*) M. Dukši, D. Baretić, V. Čaplar and I. Piantanida, *Eur. J. Med. Chem.*, 2010, **45**, 2671; (*b*) M. Dukši, D. Baretić and I. Piantanida, *Acta Chim. Slov.*, 2012, **59**, 464.
23 A. Rodger and B. Norden, *Circular Dichroism and Linear Dichroism*, Oxford University Press, New York, 1997, ch. 2.
24 N. Berova, K. Nakanishi and R. W. Woody, *Circular Dichroism Principles and Applications*, Wiley-VCH, New York, 2nd edn, 2000.
25 M. Eriksson and B. Nordén, *Methods Enzymol.*, 2001, **340**, 68.
26 (*a*) G. Scatchard, The attractions of proteins for small molecules and ions, *Ann. N.Y. Acad. Sci.*, 1949, **51**, 660; (*b*) J. D. Mc Ghee and P. H. von Hippel, Theoretical aspects of DNA-protein interactions: Co-operative and non-co-operative binding of large ligands to a one-dimensional homogeneous lattice, *J. Mol. Biol.*, 1974, **86**, 469.
27 M. Demeunynck, C. Bailly and W. D. Wilson, *Small Molecule DNA and RNA Binders: From Synthesis to Nucleic Acid Complexes*, Wiley-VCH Verlag GmbH & Co. KGaA, 2004.

28 E. Garcia-Espana, I. Piantanida and H. J. Schneider, *Nucleic Acids as Supramolecular Targets*, Royal Society of Chemistry, London, 2013.
29 A. Cheguillaume, A. Salau, S. Sinbandhit, M. Potel and P. Gall, *J. Org. Chem.*, 2001, **66**, 4923.
30 A. Salaün, A. Favre, B. Le Grel, M. Potel and P. Le Grel, *J. Org. Chem.*, 2006, **71**, 150.
31 G. Lelais and D. Seebach, *Helv. Chim. Acta*, 2003, **86**, 4152.
32 K. Gröger, D. Baretić, I. Piantanida, M. Marjanović, M. Kralj, M. Grabar, S. Tomić and C. Schmuck, *Org. Biomol. Chem.*, 2011, **9**, 198.
33 W. Humphrey, A. Dalke and K. Schulten, VMD - Visual Molecular Dynamics, *J. Mol. Graphics*, 1996, **14**, 33.
34 C. R. Cantor and P. R. Scimmel, *Biophysical Chemistry*, WH Freeman and Co., San Francisco, 1980, vol. 3, pp. 1109–1181.
35 R. Günther and H. J. Hofmann, *J. Am. Chem. Soc.*, 2001, **123**, 247.
36 W. S. Horne and S. H. Gellman, *Acc. Chem. Res.*, 2008, **41**, 1399.
37 T. A. Martinek and F. Fülöp, *Chem. Soc. Rev.*, 2012, **41**, 687.
38 S. H. Choi, I. A. Guzei, L. C. Spencer and S. H. Gellman, *J. Am. Chem. Soc.*, 2009, **131**, 2917.
39 W. S. Horne, L. M. Johnson, T. J. Ketas, P. J. Klasse, M. Lu, J. P. Moore and S. H. Gellman, *Proc. Natl. Acad. Sci. U. S. A.*, 2009, **106**, 14751.
40 Z. Hegedüs, E. Wéber, E. Kriston-Pál, I. Makra, A. Czibula, E. Monostori and T. A. Martinek, *J. Am. Chem. Soc.*, 2013, **135**, 16578.
41 B. J. Smith, E. F. Lee, J. W. Checco, M. Evangelista, S. H. Gellman and W. D. Fairlie, *ChemBioChem*, 2013, **14**, 1564.
42 H. S. Haase, K. J. Peterson-Kaufman, S. K. Lan Levengood, J. W. Checco, W. L. Murphy and S. H. Gellman, *J. Am. Chem. Soc.*, 2012, **134**, 7652.
43 L. Nevola and E. Giralt, *Chem. Commun.*, 2015, **51**, 3302.
44 L.-M. Tumir, M. Radić Stojković and I. Piantanida, *Beilstein J. Org. Chem.*, 2014, **10**, 2930.
45 L.-M. Tumir, M. Radić-Stojković and I. Piantanida, *Beilstein J. Org. Chem.*, 2014, **10**, 2930–2954.
46 (*a*) J. Lhomme, J. F. Constant and M. Demeunynck, *Biopolymers*, 1999, **52**, 65–83; (*b*) A. Martelli, J. F. Constant, M. Demeunynck, J. Lhomme and P. Dumy, *Tetrahedron*, 2002, **58**, 4291.
47 B. M. Zeglis, J. A. Boland and J. K. Barton, *Biochemistry*, 2009, **48**, 839–849.
48 S. M. Butterfield, W. J. Cooper and M. L. Waters, *J. Am. Chem. Soc.*, 2005, **127**, 24–25.
49 S. T. Meyer and P. J. Hergenrother, *Org. Lett.*, 2009, **11**, 4052–4055.
50 H. J. Xi, D. Gray, S. Kumar and D. P. Arya, *FEBS Lett.*, 2009, **583**, 2269–2275.
51 J. B. Chaires, N. Dattagupta and D. M. Crothers, *Biochemistry*, 1982, **21**, 3933.
52 G. Malojčić, I. Piantanida, M. Marinić, M. Žinić, M. Marjanović, M. Kralj, K. Pavelić and H.-J. Schneider, *Org. Biomol. Chem.*, 2005, **3**, 4373.
53 C. Ciatto, M. L. D'Amico, G. Natile, F. Secco and M. Venturini, *Biophys. J.*, 1999, **77**, 2717.
54 A. Das, K. Bhadra, B. Achari, P. Chakraborty and G. S. Kumar, *Biophys. Chem.*, 2011, **155**, 10.
55 I. Piantanida, B. S. Palm, M. Žinić and H.-J. Schneider, *J. Chem. Soc., Perkin Trans. 2*, 2001, 1808.
56 J. L. Mergny and L. Lacroix, *Oligonucleotides*, 2003, **13**, 515.

